CHAPTER IV

RESULTS AND DISCUSSION

In this chapter, the results were obtained from colorimetric detection based on GSH and Cys modified AgNPls for detecting Ni(II). The discussion was described including the optimization of the operating condition and analytical performance. In the following sections, the proposed method was successfully applied to determine Ni(II) in gold plating solution from jewelry factory and compared with conventional method like ICP-OES technique.

4.1 Characterization of GSH-Cys-AgNPls

To investigate the modification of GSH and Cys on the AgNPls surface, FTIR and UV-vis spectroscopy were respectively performed. Figure 4.1 shows the comparison of infrared spectra between pure GSH, pure Cys and GSH-Cys-AgNPls. The characteristic peak of –SH at 2522 and 2549 cm^{-1} in pure GSH and Cys had significantly disappeared in the FT-IR spectra of GSH-Cys-AgNPls. This result indicated that GSH and Cys were successfully modified onto the surface of AgNPls via the –SH group of these compounds, corresponding to similar result in the previous literature report [58].

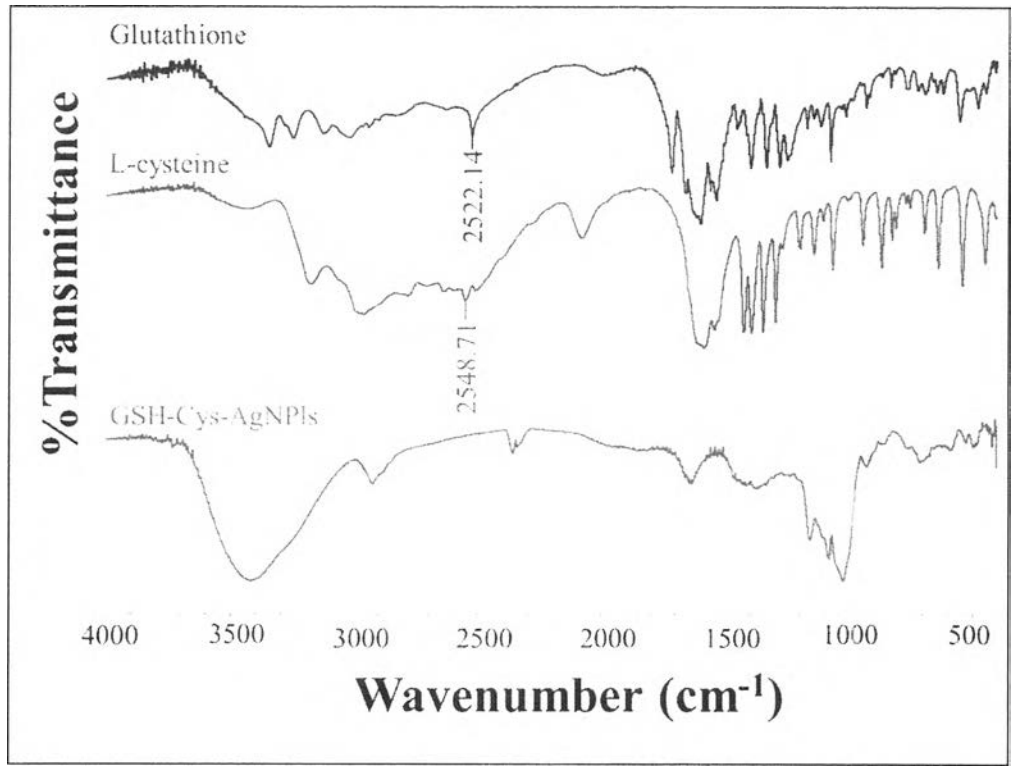

Figure 4.1 FTIR spectra of pure GSH, pure Cys and GSH-Cys modified AgNPls.

The UV-vis spectra in Figure 4.2 revealed that the localized surface plasmon resonance (LSPR) absorption peak of AgNPls was shifted from 487 nm to 501 nm after adding the GSH and Cys modifier. The red-shifted band is mainly caused by the reduction of the plasma oscillation frequency around the nanoparticles due to the binding between thiol-containing compounds and the metal nanoparticles [59].

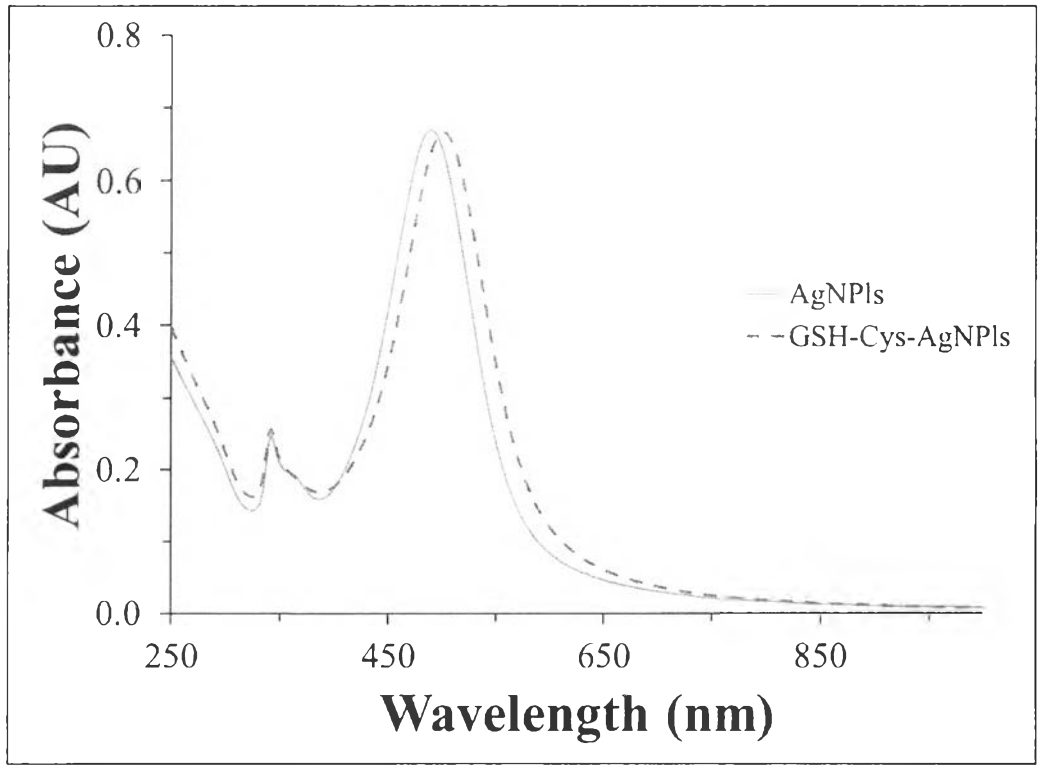

Figure 4.2 Absorption spectra of unmodified AgNPls and GSH-Cys modified AgNPls in aqueous solution.

4.2 GSH-Cys-AgNPls based colorimetric detection of nickel

After the synthesis and modification of AgNPls, the colorimetry sensor using GSH-Cys-AgNPls for the detection of Ni(II) was performed. At the beginning, GSH-Cys-AgNPls was well dispersed in pink-colored solution. After the addition of Ni(II), the color visibly changed to purple immediately presumably due to the aggregation of GSH-Cys-AgNPls induced by Ni(II) as schematically demonstrated in Figure 4.3. The aggregated solution of Ni(II) and GSH-Cys-AgNPls was tested by UV-vis spectroscopy. The UV-vis spectra were obtained as shown in Figure 4.4.

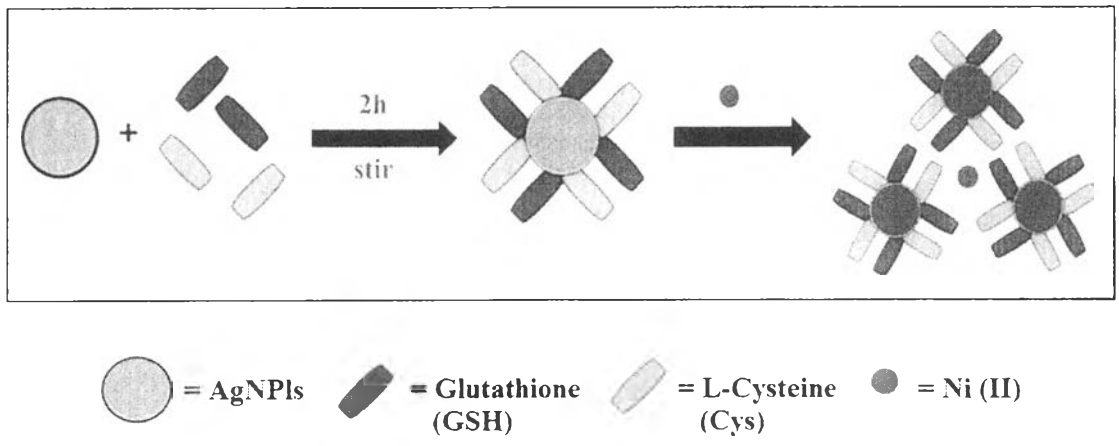

Figure 4.3 Schematic of modification and aggregation process of AgNPls.

From the UV-vis spectra, the single absorption peak of GSH-Cys-AgNPls (blue line) was observed at the maximum wavelength of 501 nm, ascribed to the LSPR absorption of GSH-Cys-AgNPls. The formation of GSH-Cys-AgNPls aggregates induced by the addition of Ni(II) exhibited a decrease in the LSPR absorption peak at 501 nm and formed a new absorption band at 618 nm (red line), and the resulting color of GSH-Cys-AgNPls solution clearly changed to purple immediately. The change in color and wavelength suggested that the mixture of GSH and Cys can induce to occur the aggregation of AgNPls in the presence of Ni(II) [60].

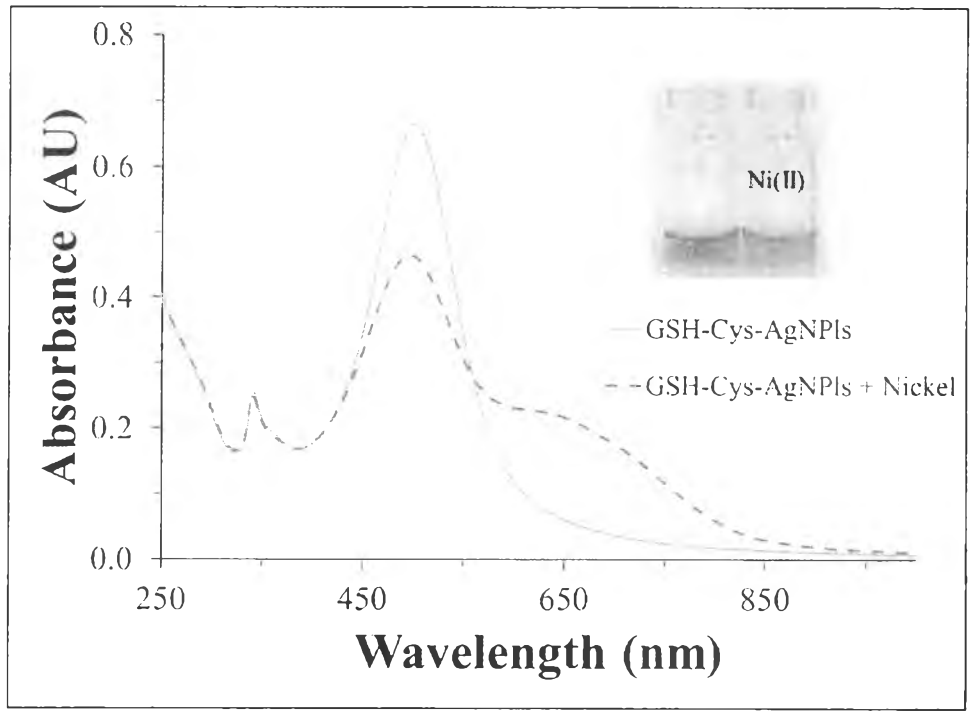

Figure 4.4 Absorption spectra of dispersed GSH-Cys-AgNPls (solid) and aggregated GSH-Cys modified AgNPls induced by the addition of Ni(II) (dash).

4.3 Characterization of Ni-GSH-Cys-AgNPls aggregates

GSH-Cys AgNPls in the presence and absence of Ni(II) were investigated using TEM. The TEM image inFigure 4.5(a) showed that, the GSH-Cys-AgNPls were nearly spherical and uniformly distributed with the average particle size in the range of roughly 30 nm. After the Ni(II) addition, the apparent aggregation of GSH-Cys-AgNPls by Ni(II) was observed (Figure 4.5(b)). These images clearly confirm the aggregation of AgNPls by Ni(II) and the increase of particle size that was postulated earlier by the change or color and the red shift of absorption wavelength.

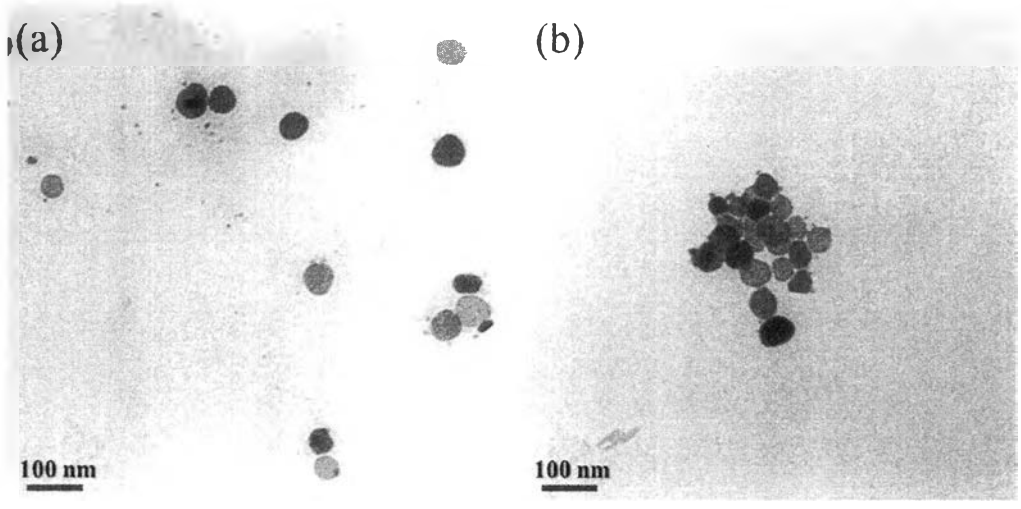

Figure 4.5 TEM images of (a) dispersed GSH-Cys-AgNPls and (b) aggregated GSH-Cys modified AgNPls induced by the addition of Ni(II).

4.4 Optimization of the modifier ratio

As the aggregation capability between Ni(II) and GSH-Cys-AgNPls is directly affected by the modifier ratio, the modifier concentration in different proportions (0.5-10 μM) was optimized. Table 4.1 and Figure 4.6 shows colors of the AgNPls solution containing various ratios of GSH and Cys.

Table 4.1 Various GSH and Cys ratios on the modification of AgNPls.

Cys \ GSH	0.1	0.5	1	5	10
0.1	Label #1	Label #2	Label #3	Label #4	Label #5
0.5	Label #6	Label #7	Label #8	Label #9	Label #10
1	Label #11	Label #12	Label #13	Label #14	Label #15
5	Label #16	Label #17	Label #18	Label #19	Label #20
10	Label #21	Label #22	Label #23	Label #24	Label #25

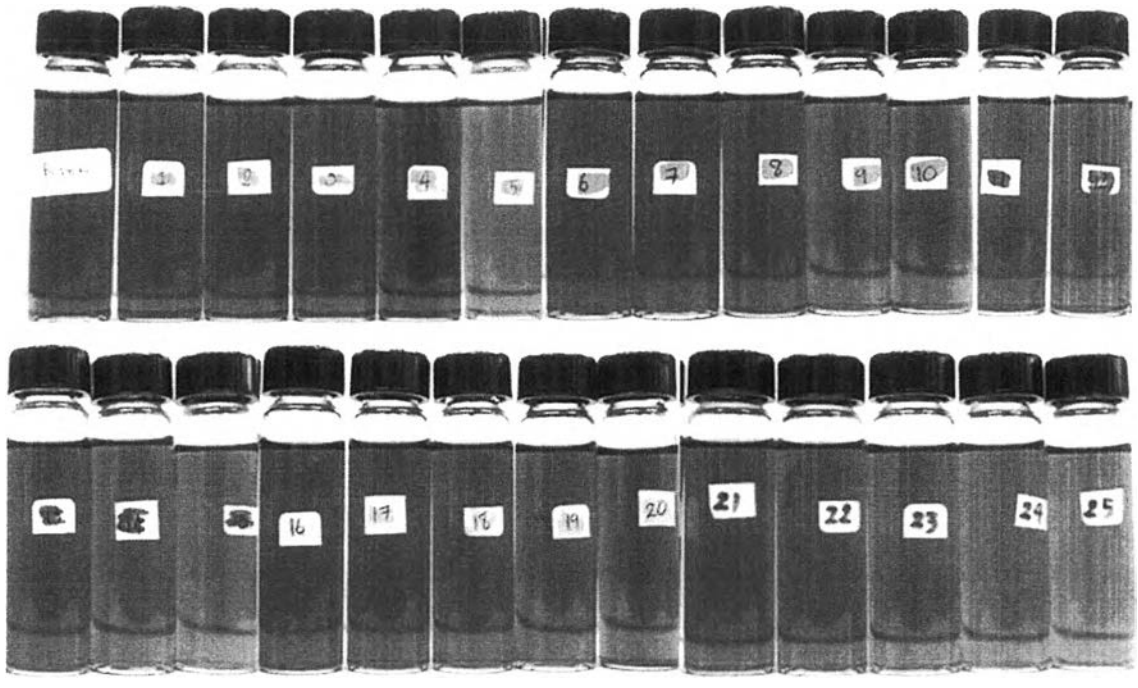

Figure 4.6 Photographs of AgNPls modified by various ratios of GSH and Cys.

After the bare AgNPls was modified by using various concentration of GSH and Cys, the resulting color of modified AgNPls solution was clearly distinguished. As shown in Figure 4.6, the obtained AgNPls solution can be categorized into 3 colors such as pink, orange, and purple. Originally, the color of bare AgNPls solution is pink. However, if the excess GSH and Cys concentration was used, the color of AgNPls solution was changed to orange and purple. The change of color to orange after the modification step suggested that the AgNPls size might be reduced. The purple solutions could be an indication that the self-aggregation of AgNPls without adding Ni(II) took place [61]. As an important concept in the surface modification of nanoparticle, the color solutions after modification should be similar to the color of original nanoparticle solutions. Therefore, only the modified solution in the range of 0.5 – 5 μM of GSH and Cys concentration was selected and used for the further experiments.

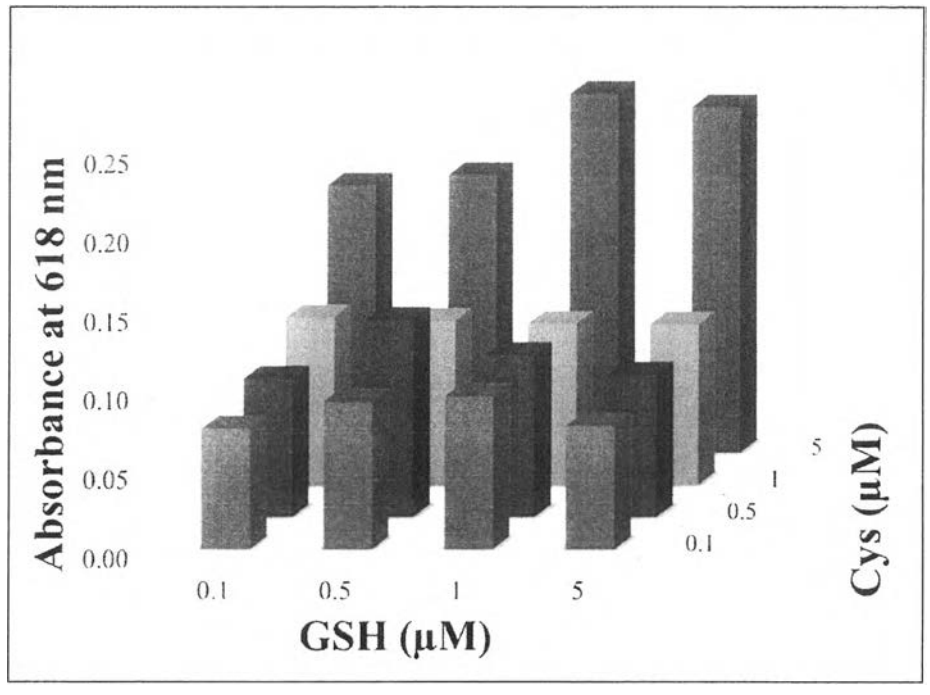

Figure 4.7 Effect of GSH and Cys ratio on the modification of AgNPls for the detection of Ni(II) using absorbance at 618 nm.

From Figure 4.7 revealed that the highest absorbance at 618 nm was obtained using GSH and Cys concentration ratio equal 1:5, distinguishing clearly from the other GSH and Cys proportions. We believe that this optimal GSH and Cys ratio provides greater aggregation via the interaction between Ni(II) and a suitable surface modification of GSH-Cys-AgNPls [62].

4.5 Optimization of pH

The influence of pH over the range of 2.5 to 11.0 on the aggregation process was studied. As shown in Figure 4.8, in pH 7.0 and 8.0, the aggregation was readily attained as clearly indicated by its increasing absorbance at 618 nm. Although the phosphate buffer pH 7.0 provided the highest intensity, the selectivity towards the Ni(II) detection was enormously decreased (Figure 4.9). Interestingly, at pH 8.0, intensive absorbance

from Ni-GSH-Cys-AgNPls was observed while a negligible response from other metal ions was found. This result implies that GSH-Cys-AgNPls at pH 8 can be utilized for selectively binding with Ni(II), forming greater aggregation than other metal species.

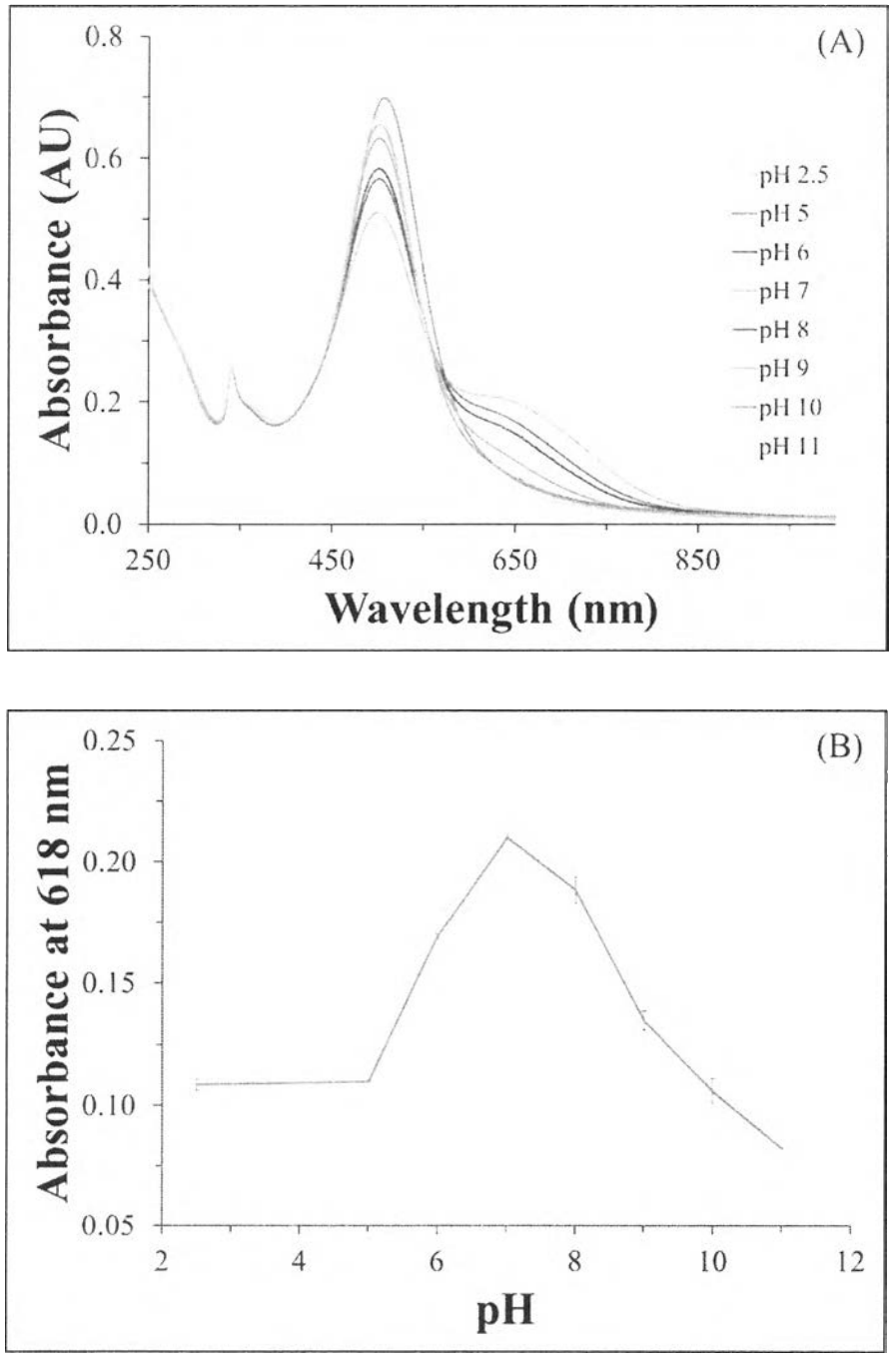

Figure 4.8 (A) UV–vis spectra and (B) Absorbance at 618 nm of GSH-Cys–AgNPls solutions with different pH ranging from 2.5 to 11.0 when adding Ni(II) solution.

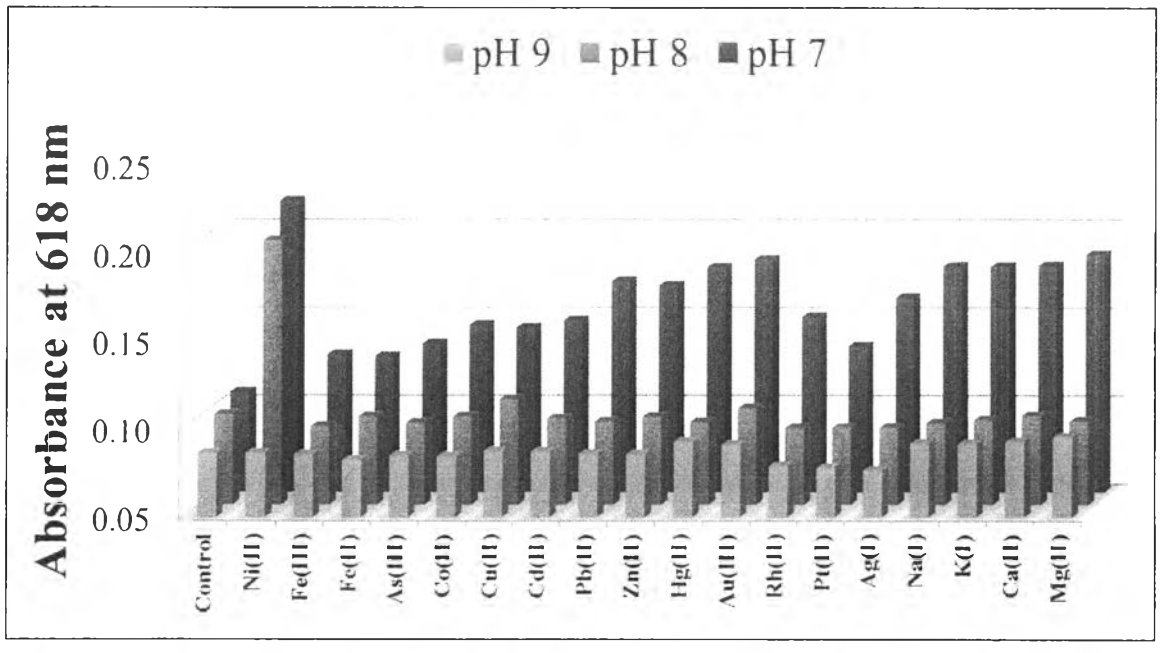

Figure 4.9 pH effect on selectivity towards Ni(II) detection in the presence of other metals.

4.6 Optimization of incubation times

Another important control in the aggregation between GSH-Cys-AgNPls and Ni(II) is the reaction times. As shown in Figure 4.10, the different incubation times lead to a different aggregation response in terms of the change in the optical spectra. The kinetics between GSH-Cys-AgNPls and Ni(II) was evaluated from a plot of absorbance vs. incubation times. The result indicated that the absorbance of GSH-Cys-AgNPls at 618 nm increased and became steady within approximately 6 min.

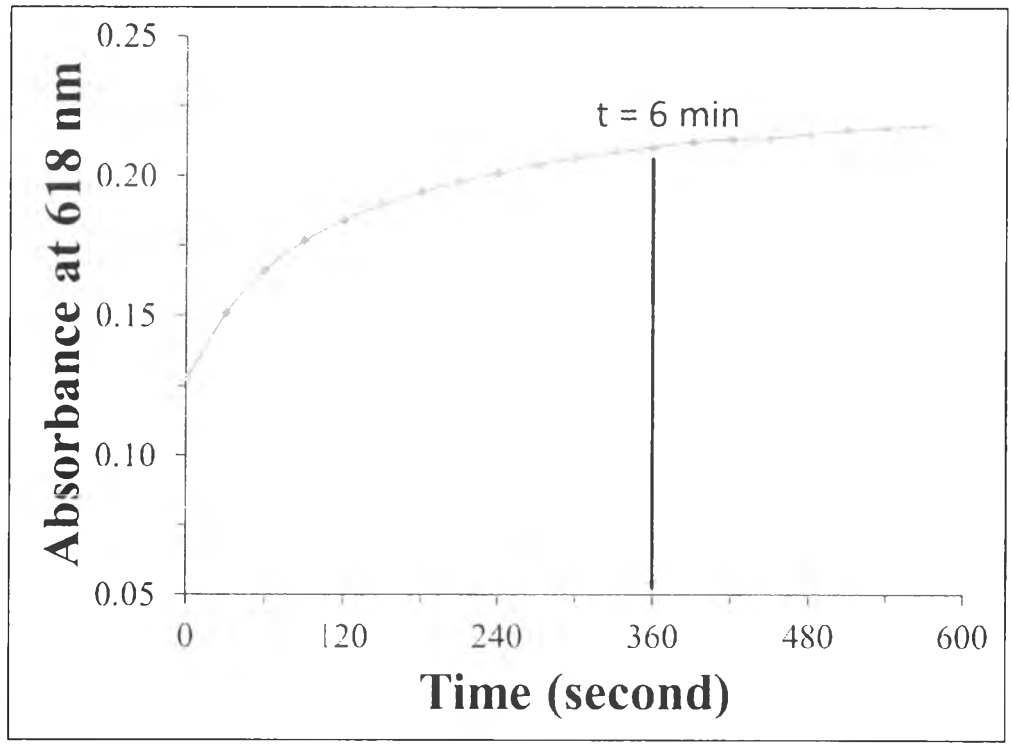

Figure 4.10 Effect of incubation time on absorbance at 618 nm of GSH-Cys-AgNPls with the presence of Ni(II).

4.7 Selectivity of GSH-Cys-AgNPls toward Ni(II) detection

The selective responses for Ni(II) detection using the proposed sensor, depending on the functional group of modifier. The functional groups or ligands containing lone pair electron in the structure of GSH and Cys such as $-NH_2$, –COOH can easily bind with Ni(II) [63]. However, the specific conditions to achieve the selective detection of Ni(II) including pH solution and modifier ratio might be required.

To investigate the selectivity of this method, various concentrations of other foreign metal ions including Fe(III), Fe(II), As(III), Co(II), Cu(II), Cd(II), Pb(II), Zn(II), Hg(II), Au(III), Rh(II), Pt(II), Ag(I) (transition-metal ions), Na(I), K(I) (alkali), Mg(II), Ca(II) (alkaline earth) were studied under the optimal conditions. The UV-vis spectra and photo images

of GSH-Cys-AgNPls containing Ni(II) along with other metals were shown in Figure 4.11 and Figure 4.12. The results demonstrated that only Ni(II) induced a remarkable aggregation of GSH-Cys-AgNPls while no significant response was observed from other metal ions.

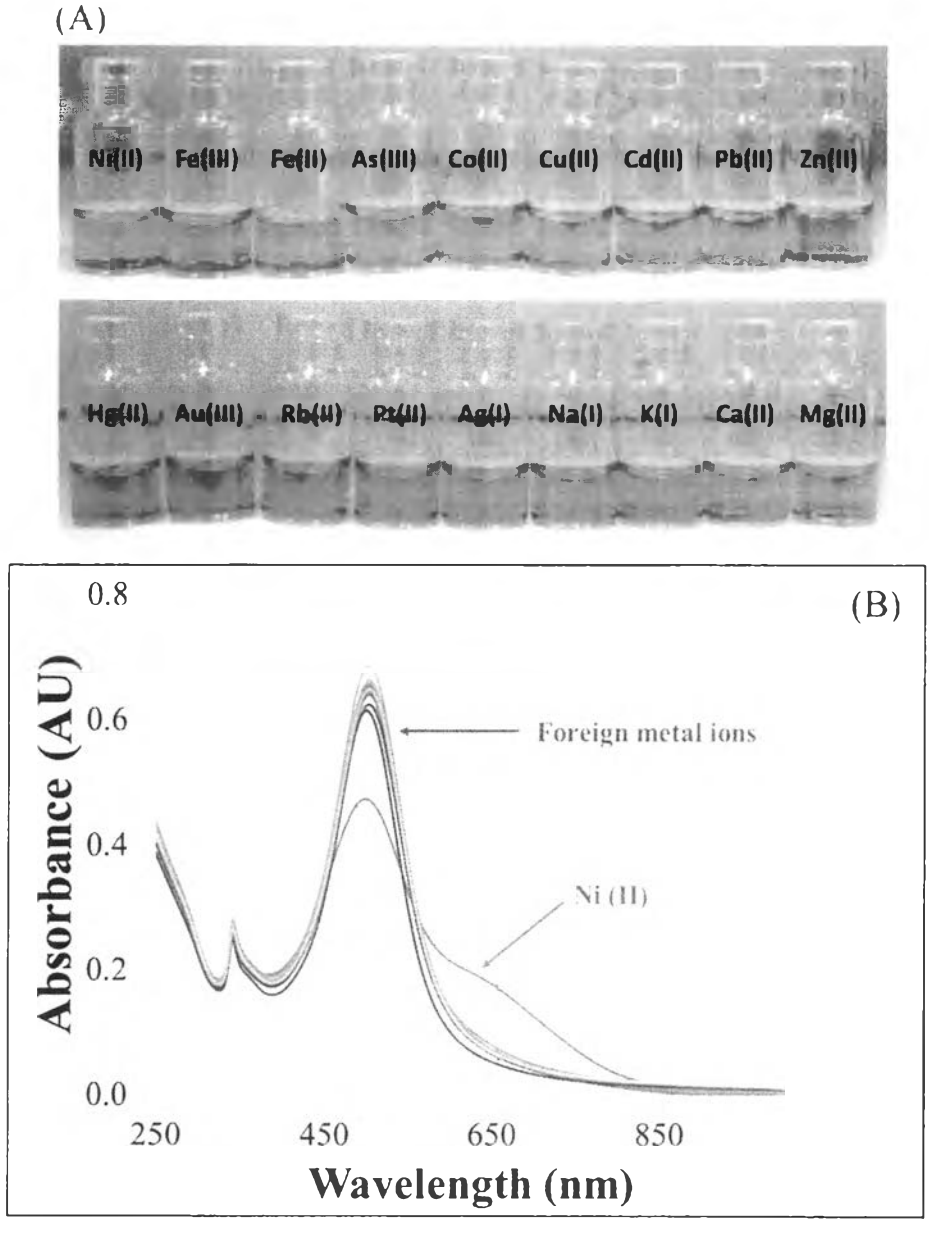

Figure 4.11 (A) Photographs, (B) UV–vis spectra of GSH-Cys-AgNPls contained with various metal ions including Fe(II), Fe(III), As(III), Co(II), Cu(II), Cd(II), Pb(II), Zn(II), Hg(II), Au(III), Rh(II), Pt(II), Ag(I), Na(I), K(I), Ca(II), Mg(II).

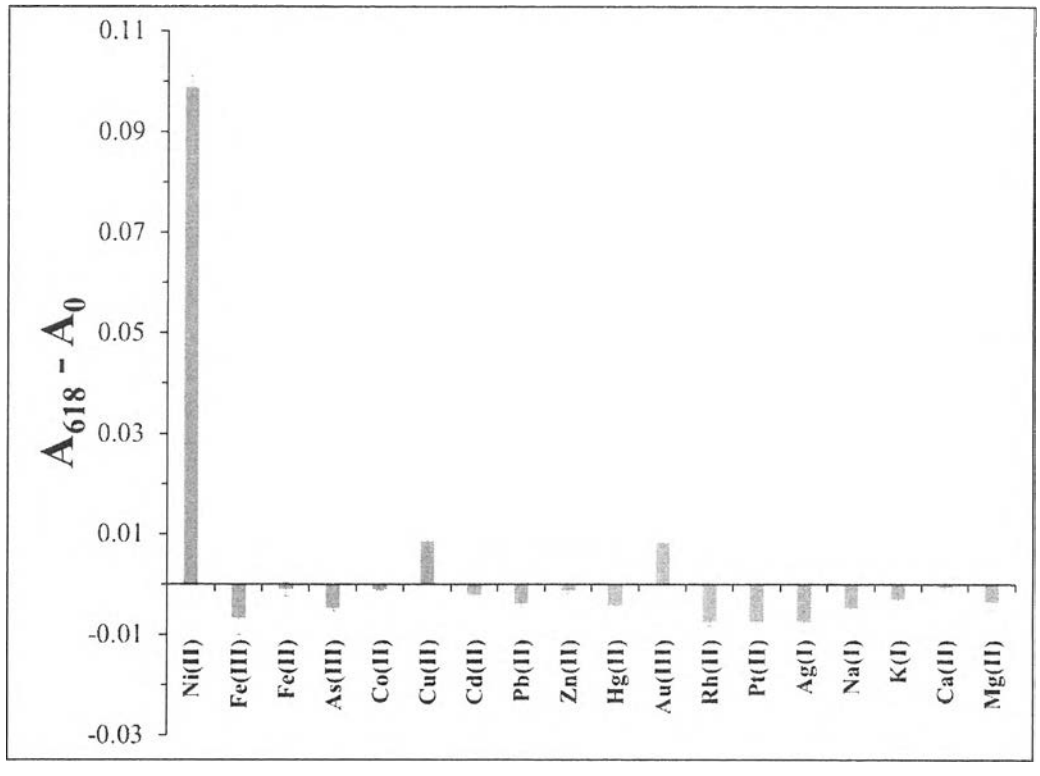

Figure 4.12 The comparison of subtracted absorbance of GSH-Cys modified AgNPls in the presence of Ni(II) and other foreign metals.

In addition, the tolerance concentration of interfering metal ions on the Ni(II) determination using the present colorimetric sensor are shown in the

Table 4.2. This tolerance limit was defined as the concentration of interfering metal ions that produces a change in absorbance of ± 5% of the analyte. According to the results, it can be seen that the interference effects from almost all metal ions did not affect Ni(II) detection. Nevertheless, only Pt(II) probably impacted the reliability and sensitivity of the proposed colorimetric sensor. Thus, it should be noted that the possible interfering ions like Pt(II) needed to be removed, masked or even diluted to a level that no longer influenced the analytical findings.

Table 4.2 Tolerance ratio of interfering ions in the determination of Ni(II) 70 ppb.

Interferences	Tolerance concentration of interfering ion (ppb)	Tolerance ratio ($C_{ions}/C_{Ni(II)}$)
Rh(II), Ag(I), Ca(II)	4690	64
Zn(II), Fe(III), Mg(II), K(I)	1120	16
Hg(II), Na(I)	560	8
Cu(II), Fe(II), Au(III), Co(II), As(III), Cd(II), Pb(II)	280	4
Pt(II)	140	2

4.8 Analytical performance

4.8.1 Calibration curve

The calibration curve was obtained from UV-vis spectra (Figure 4.13) of GSH-Cys-AgNPls solution with added concentrations of Ni(II) at incubation time of 6 min. With the increase of Ni(II) concentration, the absorbance of GSH-Cys-AgNPls at 501 nm was significantly reduced while an absorption peak of aggregated Ni-GSH-Cys-AgNPls at 618 nm was dramatically increased. In Figure 4.14, a linear relationship between the absorbance at 618 nm and Ni(II) concentration was established. Absorbance of Ni-GSH-Cys-AgNPls at 618 nm is directly proportional to the added Ni(II) concentration. A good linearity was observed in the concentration range of 10 ppb to 150 ppb Ni(II) with a correlation coefficient of 0.9971.

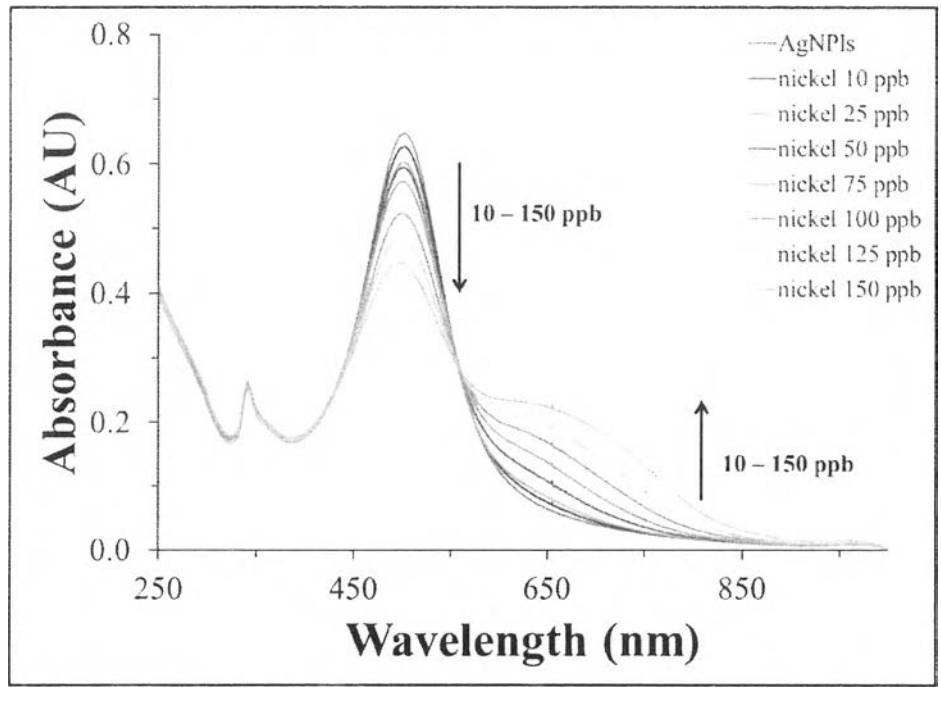

Figure 4.13 The UV–vis spectra of GSH–Cys-AgNPls solutions with various concentrations of Ni(II) ranging from 10 to 150 ppb with incubation time: 6 min.

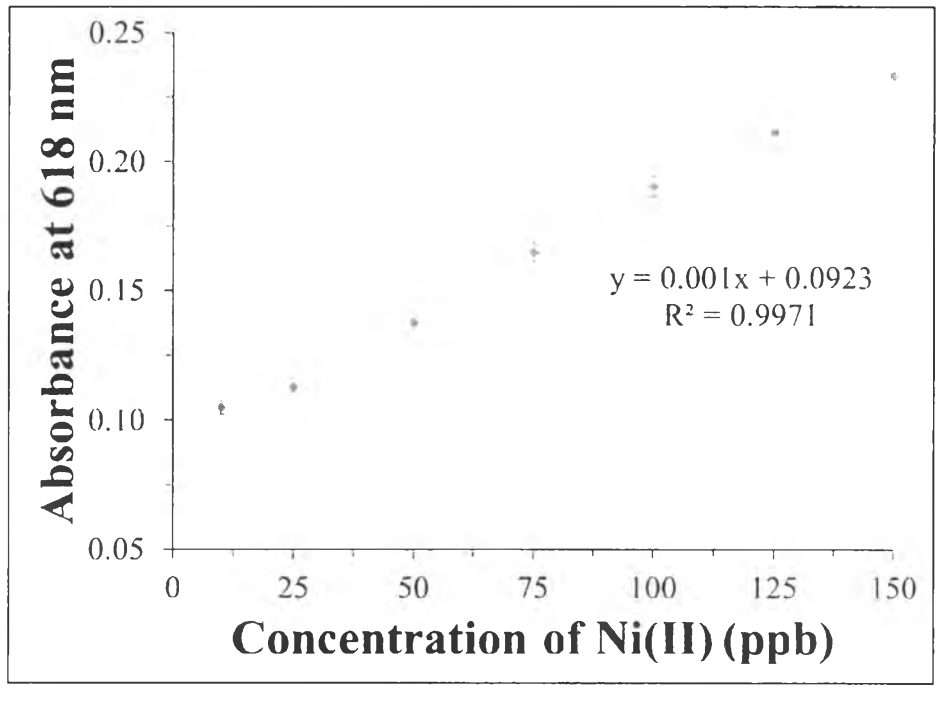

Figure 4.14 Calibration plot of the absorbance at 618 nm versus various Ni(II) concentrations including 10 ppb, 25 ppb, 50 ppb, 75 ppb, 100 ppb, 125 ppb, and 150 ppb.

4.8.2 The limit of detection (LOD) and the limit of quantitation (LOQ)

The limit of detection (LOD) and the limit of quantitation (LOQ) for Ni(II) ions were found to be 7.02 ppb (S/N=3) and 23.01 ppb (S/N=10), respectively. The performance of the colorimetric GSH-Cys-AgNPls sensor was compared to the other colorimetric nanoparticle sensors used for Ni(II) detection as shown in Table 4.3. It is clear that our sensor shows a relatively high colorimetric sensitivity and superior LOD for Ni(II) detection.

Table 4.3 The comparison of analytical performance of different colorimetric methods using modified metal nanoparticle for the determination of Ni(II).

Colorimetric sensor	Linear range	Detection limit	Reference
GSH-AgNPs	58.7 ppb - 58.7 ppm	4.4 ppm	[54]
NAC-AgNPs	0 -1.17 ppm 1.17 – 2.82 ppm	13.5 ppb	[56]
AuNPs-NTA/AuNPs-L-carnosine	0 - 250 ppb	30 ppb	[55]
GSH-Cys-AgNPls	10 - 150 ppb	7.02 ppb	This work

Abbreviations: GSH, glutathione; AgNPs, silver nanoparticles; NAC, N-acetyl-L-cysteine; AuNPs, gold nanoparticles; NTA, nitrilotriacetic acid; Cys, L-cysteine; AgNPls, silver nanoplates.

4.8.3 Repeatability

In this work, the repeatability was studied by performing eleven repeated measurements of standard nickel solution. The colorimetric GSH-Cys-AgNPls sensor

showed high repeatability within 5% RSD in different concentrations, as shown in Figure 4.15 and

Table 4.4.

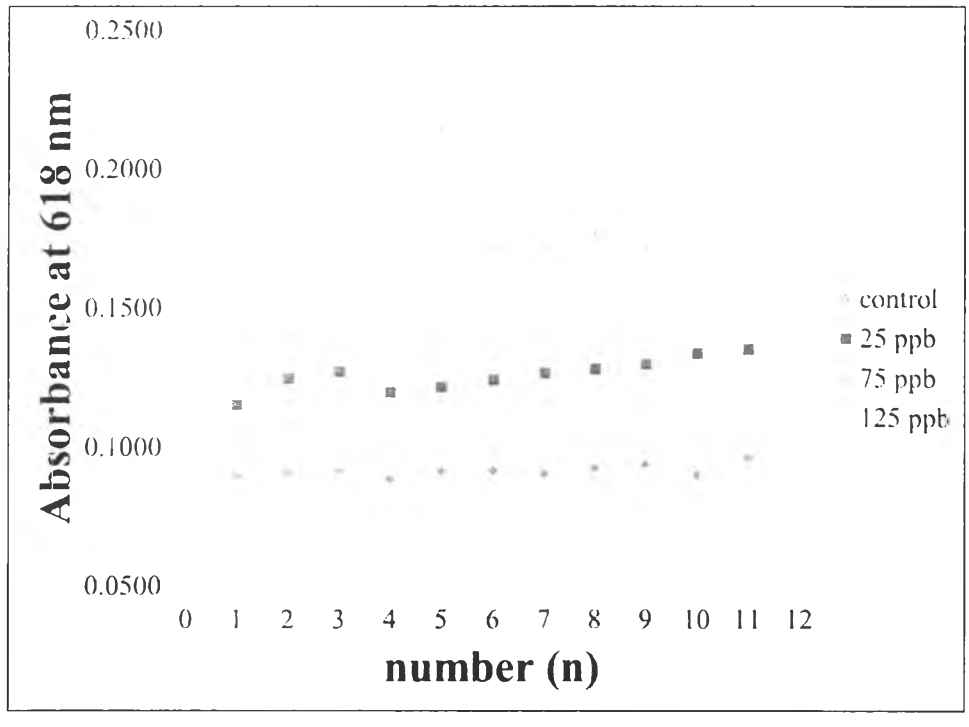

Figure 4.15 The stability of absorption spectra at 618 nm using colorimetric GSH-Cys-AgNPls sensor for detecting Ni(II) in optimal condition (GSH : Cys = 1:5, phosphate buffer pH 8.0 ,and incubation time 6 min).

Table 4.4 The relative standard deviations of colorimetric GSH-Cys-AgNPls sensor for detecting Ni(II) (n=11).

Concentration of Ni(II)	SD	%RSD
25 ppb	0.005898	4.6745
75 ppb	0.002418	1.3880
125 ppb	0.004579	2.1829

4.9 Analytical application in a real sample

To evaluate the efficiency of our method, the colorimetric GSH-Cys-AgNPls sensor was used to detect Ni(II) in gold-plating solution of a jewelry factory. Under the optimal conditions, the gold-plating solution was determined using external standard quantitation method. The level of Ni(II) in samples 1 and 2 were found to be 50.00 ± 2.73 and 57.33 ± 0.60 ppb, respectively (n = 3). The results of this proposed method were validated by ICP-OES method. Levels of Ni(II) in samples 1 and 2 were in good agreement (98.85% and 96.18%, respectively) with the values obtained from ICP-OES of 49.43 ± 0.95 and 55.22 ± 0.11 ppb, respectively. As a result, this proposed colorimetric sensor can be applied for the selective Ni(II) determination of the gold-plating solution samples with satisfactory results.